1 1 Introduction

2

3 More than half of the Earth's land surface has been affected by land use and land cover change 4 (LULCC) activities over the last 300 years, largely from the expansion of agriculture (Hurtt et al., 2011), 5 leading to numerous climate impacts (Foley et al., 2005). Conversion of land from natural vegetation to agriculture or pasturage releases carbon from vegetation and soils into the atmosphere (Houghton et al. 6 7 1983), often quickly through fires, which emit carbon dioxide (CO_2), methane (CH_4), ozone (O_3)-8 producing compounds and aerosols (Randerson et al., 2006). Deforested areas have a diminished 9 capacity to act as a CO₂ sink as atmospheric CO₂ concentrations increase (Arora and Boer, 2010; 10 Strassmann et al., 2008). Furthermore, agriculture and pasturage emits CH₄ and nitrous oxide (N₂O), 11 accelerates soil carbon loss (Lal, 2004), and changes aerosol emissions (Foley et al., 2011). For 12 instance, land management can enhance mineral dust aerosol emission by modifying surface sediments 13 and soil moisture (Ginoux et al., 2012), but reduces fire aerosol emissions (Kloster et al., 2012) and 14 emissions of low-volatility products of oxidized biogenic organic compounds that condense to form 15 secondary organic aerosols (SOA; Heald et al., 2008). Changes in the abundance of these atmospheric 16 constituents generate forcings onto the climate system (Fig. 1), quantified in this study as radiative forcings (RF). 17

18

19 The global RF and associated climate response attributable to LULCC are often portrayed as a balance between cooling biogeophysical effects (changes in surface energy and water balance) and the warming 20 biogeochemical effect of increases in atmospheric CO₂ (e.g. Claussen et al., 2001; Brovkin et al., 2004; 21 22 Foley et al., 2005; Bala et al., 2007; Cherubini et al., 2012). Claussen et al. (2001) found that the 23 cooling from biogeophysical effects of land cover change dominated over the warming from associated CO₂ emissions in high-latitude regions where the land may be snow covered for part of the year. 24 25 whereas tropical LULCC leads to a warming due to a weaker albedo forcing. This regional contrast in 26 the dominant forcing from deforestation also applies to natural forest disturbances (O'Halloran et al., 27 2011). On a global scale, model estimates have shown both canceling climate responses to historical 28 land cover change biogeophysical effects and CO₂ emissions (Brovkin et al., 2004; Sitch et al., 2005) 29 and a net warming (0.15°C) from the same effects (Matthews et al., 2004).

30

1 Additional LULCC forcings are often grouped together with fossil fuel burning and other activities for 2 assessment of the total anthropogenic RF (e.g. Forster et al., 2007; Myhre et al., 2013). Nevertheless, there is some recognition of the importance of evaluating emissions of non-CO₂ greenhouse gases 3 4 attributable to LULCC separately from fossil fuel emissions for targeting emission reduction policies 5 (Tubiello et al., 2013). Less attention is given to forcings from short-lived atmospheric species that are 6 affected by LULCC. Foley et al. (2005) acknowledge that changes in the concentrations of short-lived 7 species, aerosols and O₃, attributable to LULCC are important for air quality assessment but do not 8 estimate the impacts of these species on climate. Unger et al. (2010) partition sources of global, 9 anthropogenic RF into economic sectors, including agriculture. They consider non-CO₂ greenhouse gas and aerosol forcing agents but only for present day land use emissions and they do not include land 10 11 cover change. The full contribution of LULCC to global RF compared to the contribution from other 12 anthropogenic activities remains unquantified.

13

14 Here we compute the CO₂ and albedo RF attributable to global LULCC and compare to previous 15 estimates of these values, but we also compute the forcings from non-CO₂ greenhouse gases (CH₄, N₂O, 16 O₃), and aerosol effects (direct, indirect, deposition on snow and ice surfaces). Individual forcings are computed from the results of terrestrial model simulations forced with historical land cover changes and 17 18 wood harvesting, and projected land cover changes from five future scenarios. Because the land model 19 used here includes a carbon model, fire module and emissions of volatile organic compounds, we can 20 uniquely account for the complicated interplay between land use and fire (e.g. Marlon et al., 2008, 21 Kloster et al., 2010; Ward et al., 2012). Four of the future scenarios of land cover change correspond to 22 the four Representative Concentration Pathways (RCP) that were developed for the Climate Model Intercomparison Project in preparation for the IPCC 5th assessment report (AR5) (Lawrence et al., 2012; 23 24 Hurtt et al., 2011; van Vuuren et al., 2011). The low emissions scenario, RCP2.6, includes widespread 25 proliferation of bioenergy crops, while RCP4.5 is characterized by global reforestation as a result of 26 carbon credit trading and emission penalties (Hurtt et al., 2011). The higher emissions scenarios include 27 expansion of crop area at the expense of existing grasslands (RCP6.0; Fujino et al., 2006) or forests 28 (RCP8.5; Riahl et al., 2007) (Hurtt et al., 2011). We introduce a fifth, more extreme scenario, in which 29 all arable and pasturable land is converted to agricultural land, either for crops or pasture, by the year 30 2100. This scenario, hereafter referred to as the theoretical extreme case (TEC), was not developed 31 within an integrated modeling framework and, therefore, its likelihood of occurrence given economical

and additional environmental constraints is difficult to judge. Instead, this scenario gives a theoretical
 upper bound on LULCC impacts over this century. The range in outcomes for the RF attributable to
 LULCC based on these five projections strengthens our understanding of the role that LULCC decision making will play in future climate.

5

6 2 Overview of methods

7

8 Our approach for computing the RFs begins with estimating emissions of trace gases and aerosols from 9 a diverse set of LULCC activities, many of which are illustrated schematically in Fig. 1. For several forcing agents, including CO₂, we isolate the LULCC emissions by comparing global transient 10 11 simulations of the terrestrial biosphere including LULCC to simulations without LULCC that are 12 otherwise identical, and attribute the difference in emissions between these simulations to LULCC. This general approach, attributing the differences between the LULCC and no-LULCC environment to the 13 impacts of LULCC, also applies to our calculations of RFs. Our methods for computing these and other 14 15 emissions from LULCC activities, as well as the calculations of changes in atmospheric constituent 16 concentrations and RFs are summarized in this section and schematically in Fig. 2.

17

18 **2.1 LULCC activities**

19

We model the following LULCC activities with a global terrestrial model; wood harvesting, land cover change, and changes in fire activity, including deforestation fires. Changes in the terrestrial model carbon cycle driven by the historical and projected LULCC are used to derive the RF of surface albedo change, and emissions of CO₂, SOA, smoke, and mineral dust from LULCC (Fig. 2). We assemble emissions from additional LULCC activities; agricultural waste burning, rice cultivation, fertilizer applications, and livestock pasturage, from available datasets corresponding to the RCP LULCC projections.

27

Future land cover changes and wood harvesting rates projections have been developed as part of the
Coupled Model Intercomparison Project phase 5 (CMIP5) (Taylor et al., 2012) with projections

30 corresponding to each of the four RCP scenarios (Hurtt et al., 2011; van Vuuren et al., 2011). These

31 projections have since been joined to historical reconstructions of land use (Hurtt et al., 2011) and

1 expressed as changes in fractional plant functional types (PFTs) which we use in this study with recently

2 amended wood harvesting rates for RCP6.0 and RCP8.5 (Lawrence et al., 2012). Global forest area

3 decreases in all projections between 2010 and 2100 except for RCP4.5, which projects large

4 reforestation efforts (Fig. A1). The loss in forests is accompanied by increases in global crop area in all

5 scenarios except RCP4.5 in which crop area decreases to a level not seen since the 1930s (Fig. A1).

6 Development of PFT changes for the TEC is described in Appendix A.

7

8 While we consider this list of activities to be highly inclusive, several LULCC activities and processes 9 are not included in this study, either because they are difficult to properly model or represent as a forcing, or because of a poor level of current understanding of the process. We exclude the impacts of 10 11 anthropogenic water use, mainly irrigation, on global water vapor concentrations and the associated RF 12 (Boucher et al., 2004). Changes in water use and land use have numerous other implications for the hydrological cycle including impacts on evapotranspiration, runoff, and wetland extent (Sterling et al., 13 2013). Related to these effects, the impact of land surface albedo changes may be further moderated by 14 changes in cloudiness (Lawrence and Chase, 2010), which we did not consider in this analysis. Also, 15 16 emissions of CH₄ are tied to the global extent of wetlands, which have likely changed since preindustrial times (Lehner and Doll, 2004), but the scale and distribution of the change is not yet known well enough 17 18 to be included in our model setup. We assume that natural CH₄ emissions remain unchanged from 1850 19 through 2100 for all scenarios. Finally, there is a source of CO₂ from deforestation and forest degradation in tropical peat swamp forests that has only recently been widely recognized (Hergoualc'h 20 21 and Verchot, 2011), although it is thought that contributions from this source to current global CO₂ 22 concentrations are small (Frolking et al, 2011).

23

24 **2.2 LULCC emissions (computed from CLM)**

25

Changes in terrestrial carbon storage, fire activity and biogenic trace gas emissions due to dynamic land cover are simulated using version 3.5 of the Community Land Model (CLM) (Oleson et al., 2008; Stockli et al., 2008) with active carbon and nitrogen cycles (CN) (Thornton et al., 2009) coupled to a process-based fire model (Kloster et al., 2010). This configuration of CLM simulates the complicated interplay between land use, land use change, fires, land carbon uptake and loss, and emissions of volatile organic compounts (Thornton et al., 2009; Kloster et al., 2010; Guenther et al., 2006). To isolate the impacts of LULCC we perform separate simulations for each of the LULCC dynamic PFT scenarios and
 compare it to an identical simulation with no PFT changes. All CLM simulations use 1.9-degree latitude
 by 2.5-degree longitude spatial resolution and a 30 minute timestep.

4

5 Spin-up of CLM is carried out with year 1850 land cover, which includes some anthropogenic changes. 6 Simulations of historical LULCC run from year 1850 to 2005 and future simulations from year 2006 to 7 2100. We compute forcings in the year 2010 assuming historical LULCC was extended to 2010 with 8 RCP2.6 land cover changes. We follow the methods of Kloster et al. (2012) for historical and future 9 atmospheric forcing, including meteorology, CO₂ concentrations and N deposition. Twelve future CLM simulations are run, two for each future LULCC scenario (RCP2.6, RCP4.5, RCP6.0, RCP8.5, 10 11 theoretical extreme case, and No-LULCC) forced from the atmosphere with temperature, precipitation, 12 wind, specific humidity, air pressure, and solar radiation data from the results of two fully-coupled CMIP3 simulations. The two sets of atmospheric forcing were selected for their divergent predictions of 13 14 future temperature and precipitation (Kloster et al., 2012).

15

16 2.2.1 Fires

17

18 Fire area burned in CLM is controlled by available biomass, fuel moisture and ignition events, all 19 expressed as probabilities, and adjusted by surface wind speeds (Kloster et al., 2010). Fire emissions 20 from the area burned are contingent upon the available biomass and are partly determined by PFT-21 dependent combustion completeness. In addition to wildfires, deforestation fires occur in the model and 22 are represented as an immediate release of a portion of the carbon lost during deforestation. In our analysis, deforestation fires do not impact the overall CO₂ RF but do speed up the timing of the release 23 24 of carbon that would otherwise occur by decomposition. Deforestation fires do, however, contribute 25 small amounts of CH₄, N₂O, O₃ precursor gases, and aerosols to the atmosphere that would not have 26 been released through decomposition.

27

We attribute a reduction in global burned area, both historically and in the future, to LULCC in our
simulations (for RCP4.5, which includes large scale reforestation, the reduction is only a few percent).
This result matches our current understanding of the impact of LULCC on wildfires (Kloster et al.,

31 2012; Marlon et al., 2008).

1

2 Emissions of trace gases and aerosols by wildfires and deforestation fires are derived from the CLM 3 simulations of global fire activity. We use ten-year annual average fire carbon emission output from 4 CLM, corresponding to each analysis year (1850, 2010, 2100) to reduce the influence of interannual 5 variability in fires. Emission factors are applied to the carbon emissions from fires to determine the 6 contribution of fires to the various chemical species (see Fig. 2) including NMHCs, CH₄, N₂O, NH₃, BC, 7 OC, and SO₂ (Kloster et al., 2010; Ward et al., 2012). The LULCC contribution to global fire emissions 8 of BC and OC is negative in the year 2010 (-13%), in the year 2100 for all scenarios except for RCP4.5, 9 compared to the no-LULCC CLM realization (Table 1).

10

11 2.2.2 Dust emissions

12

Agricultural activities have been linked to increased wind erosion of soils and greater dust emission in 13 semi-arid regions (Ginoux et al., 2012). To address the impact of LULCC on dust emissions we 14 15 introduce a modified soil erodibility dataset for each scenario into simulations with the Community 16 Atmosphere Model (CAM) version 5 (Liu et al., 2011). The model protocol for these simulations is 17 identical to that used to compute the aerosol forcings (see Appendix B5). For each model grid box, a 18 new soil erodibility value is set equal to the sum of the original soil erodibility and the fraction of the 19 grid box that is cultivated land. We then introduce a parameter that weights the cultivated fraction in the 20 soil erodibility computation such that the fraction of the dust flux resulting from cultivation in the year 21 2000 for eight regions (N. America, S. America, N. Africa, S. Africa, W. Asia, C. Asia, E. Asia, and 22 Australia) is comparable to recently reported, satellite-derived values for each region (Ginoux et al., 23 2012). The weighting parameter for cultivated land was tuned with three iterations of four-year global 24 atmospheric model simulations (again using the model setup described in Appendix B5), comparing the 25 results for the tuned and un-tuned soil erodibility to the Ginoux et al. (2012) estimates for each region 26 after each iteration. From this tuning we estimate reasonable weighting parameters for the cultivated 27 fraction of land in each of the eight regions. The weighting parameters are applied to the timeseries of 28 historical and projected crop area to create timeseries of soil erodibility that are modified by cultivation. 29

- 30 Ginoux et al. (2012) estimate that 25% of present day, global dust emissions are caused by
- 31 anthropogenic activities. We attribute about 20% of global dust emissions to historical LULCC (Table

1). Once these relationships between land use and dust are developed in the current climate, the natural
 dust source, along with changes in vegetation and climate are allowed to interact with the prognostic
 dust scheme to predict changes in dust concentrations (Mahowald et al., 2006; Albani et al., 2014). The
 extreme expansion of crop and pasture area in the TEC leads to more than a tripling of global dust
 emissions, from natural and human-impacted sources, by the year 2100 using this methodology (Table
 1).

7

8 2.2.3 SOA emissions

9

Biogenic emissions of isoprene, monoterpenes, carbon monoxide (CO) and methanol depend on leaf area index (LAI) and, therefore, also on LULCC. We compute biogenic trace gas emissions using an offline version of the Model of Emissions of Gases and Aerosols from Nature (MEGAN) (Guenther et al., 2006) with a forced diurnal cycle for temperature and solar radiation (Ashworth et al., 2010). The monthly average LAI output from CLM are used for each scenario to produce the biogenic emissions with LAI scaled globally such that predicted year 2000 isoprene emissions match present day global estimates from Heald et al. (2008).

17

18 Some biogenic NMHCs, notably monoterpenes and isoprene, can undergo gas to particle phase 19 transitions in the atmosphere after oxidation (Heald et al., 2008) and contribute to changes in aerosol 20 concentrations. The rate of secondary aerosol production depends on the concentrations of the gas 21 precursors, but also the oxidation capacity of the troposphere (Shindell et al., 2009). Both criteria are predicted in our atmospheric chemistry model simulations, described in Appendix B2. On a global 22 average, we estimate a negligible LULCC attributed share of biogenic SOA precursors (mainly 23 24 isoprene) in the year 2010 and attribute larger reductions to projected changes in land cover for the 25 future RCP between 6 to 16% (Table 1), similar to the results of Wu et al. (2012) for isoprene plus 26 monoterpene emissions (~10% lower with LULCC) between 2000 and 2100 using the IPCC A1B future 27 emissions scenario.

28

29 **2.2.4 CO₂ emissions**

- 30
- 31 The anthropogenic contribution to the concentration of atmospheric CO₂, used to compute the RF at

- years 2010 and 2100, depends on the history of anthropogenic CO₂ emissions up to that point. We estimate yearly LULCC emissions to the atmosphere as being equivalent to the global annual change in terrestrial carbon storage due to LULCC. Therefore, sources as well as changes to sinks of CO₂ associated with LULCC are accounted for in the CO₂ emissions. This approach is most similar to the
- 5 "D3" group of studies as defined by Pongratz et al. (2014) in which simulations with and without
- 6 LULCC are conducted with identical meteorological and atmospheric CO₂ forcing.
- 7

8 As noted in previous studies (e.g. Strassmann et al., 2008; Arora and Boer, 2010; Pongratz et al., 2009; 9 2014), this methodology does not account for the CO₂-fertilization feedback in which the CO₂ attributed to LULCC leads to greater fertilization of natural and managed vegetation and an enhanced terrestrial 10 11 carbon sink. Arora and Boer (2010) show that excluding the CO₂-fertilization feedback leads to a form of "double-counting" land carbon storage and can cause overestimates of 20th century LULCC net 12 carbon flux by about 50%. A review of the few studies estimating this feedback gives a range for the 13 14 overestimate of the net carbon flux from LULCC of 25 to 50% (Pongratz et al., 2014). However, a 15 recent model intercomparison study suggested that including nitrogen (N)-limitation dramatically 16 reduces terrestrial carbon pool sensitivity to changes in CO₂ concentration (Arora et al., 2013). Land carbon uptake in coupled models using the CN version of CLM was only 40% as sensitive to changes in 17 18 CO₂ concentration and surface temperature increases (known as the climate change feedback) compared 19 to the model used by Arora and Boer (2010). Therefore we adjusted the yearly LULCC net carbon flux 20 downward by 20% to account for the CO₂ fertilization feedback and make our calculations of CO₂ concentration increases attributed to LULCC more consistent with the "E2" group of studies as defined 21 22 by Pongratz et al. (2014), including Arora and Boer (2010), Strassmann et al. (2008) and Pongratz et al. (2009).23

24

Other model parameters, including aerosol and biogenic NHMC fluxes, depend on LAI, which would also be impacted by the different CO_2 fertilization. However, due to the non-linearity of the aerosol and ozone response we do not apply an adjustment to these RFs but note here that the magnitude of the year 28 2010 aerosol, O_3 and indirect CH_4 RFs may be small overestimates.

29

30 Our simulated net carbon flux from LULCC does not include the impacts of cultivation on soil carbon 31 amounts. Model estimates of carbon emissions from soils that have been disrupted by land use are

1 poorly constrained (Houghton, 2010) and introduce major uncertainty into estimates of the net LULCC 2 carbon flux (House et al., 2002). In a review of field studies, Guo and Gifford (2002) conclude that soil 3 carbon is increased following most conversions of natural land to pasture, and decreased following 4 conversions to cropland. Lal (2004) estimates that cultivation has caused the loss of 78 ± 12 PgC from 5 soils since 1850. Modeling studies suggest that LULCC can contribute a net loss of soil carbon 6 globally, from ~13% of total LULCC carbon emitted (Strassmann et al., 2008) to ~37% (Shevliakova et al., 2009), or a net gain as in Arora and Boer (2010). Recently, Levis et al. (2014) implemented a 7 8 cultivation parameterization that includes impacts on soil carbon and found an additional global flux of 9 0.4 PgC yr⁻¹ from soils due to crop management in recent decades.

10

11 **2.3 LULCC emissions (not computed from CLM)**

12

This section describes the sources and accompanying computations for LULCC emissions of all relevant trace gas and aerosol species not derived from the CLM simulations in this study (Fig. 2). For non-LULCC related emissions (such as those from fossil fuel burning) we use the emission inventories from the Atmospheric Chemistry and Climate Model Intercomparison Project (ACCMIP) (Lamarque et al., 2010) for historical time periods, with future emissions from RCP4.5 (Wise et al., 2009). These datasets include emissions of non-methane hydrocarbons (NMHCs), NO, NH₃, SO₂, and organic carbon (OC) and black carbon (BC) aerosols.

20

21 2.3.1 Agricultural emissions

22

23 Agricultural emissions of important trace gas species, such as NH_3 and N_2O , are not simulated by CLM. Therefore, additional emissions from LULCC activities associated with agriculture were taken from the 24 25 integrated assessment model emissions for the different RCPs (e.g. van Vuuren et al., 2011). These 26 activities are fertilizer application, soil modification, livestock pasturage, rice cultivation and 27 agricultural waste burning, and we include global, emissions of NHMCs, NO_x, CH₄, NH₃, BC, OC, and 28 SO₂ from LULCC sources are from these activities. N₂O emissions are not reported by sector for the 29 RCPs and we compute these separately (Sect. 2.3.2). The four Integrated Assessment Models (IAMs) 30 associated with the RCPs for the fifth IPCC assessment report simulate the expansion and contraction of 31 agriculture driven by the demand for food and projected land use policies, such as carbon credits for

reforestation or support of expanded biofuel crops (van Vuuren et al., 2011). The area under cultivation
and type of agricultural activities jointly determine the future distribution of agricultural emissions for
each projection (van Vuuren et al., 2007; Wise et al., 2009; Fujino et al., 2006; Riahi et al., 2007). We
use historical agricultural emissions from ACCMIP (Lamarque et al., 2010), which covers the time
period of 1850-2005 and extend the historical emissions with RCP2.6 projected emissions through year
2010 for computing LULCC RFs in the year 2010.

7

8 For the TEC, agricultural emissions are derived by scaling the RCP8.5 emissions by the difference in 9 cultivated area between the two scenarios in year 2100. First, three latitude band average (-90° to -30°, -10 30° to 30°, and 30° to 90° latitude) values of emissions of each species per unit cultivated area are 11 computed for RCP8.5, year 2100. Next, the latitude band averages are applied to the theoretical extreme 12 case cultivated area in the year 2100, requiring the assumption that the practices and intensity of 13 agriculture in the TEC are the same as in RCP8.5, and only the cultivated area changes.

14

15 **2.3.2** N₂O emissions

16

17 N₂O has both industrial and agricultural sources, in addition to a large natural source from soils and oceans. Total anthropogenic N₂O emissions have been estimated for the historical time period and 18 19 projected for RCP4.5 (Meinshausen et al., 2011a). Additional information regarding natural emissions 20 and also agricultural emissions are needed to partition the anthropogenic N₂O emissions into LULCC 21 and non-LULCC components and estimate the associated RFs. We follow the methodology of 22 Meinshausen et al. (2011b) in which the N₂O budget is balanced for a historical time period to extract 23 the natural emissions from the total anthropogenic emissions. Natural emissions of N₂O decrease from about 11 to 9 TgN (N₂O) yr⁻¹ using this method between the years 1850 and 2000. We maintain the year 24 2000 emissions, 9 TgN (N₂O) yr⁻¹, for the years 2000 to 2100. Future land cover change, particularly the 25 26 theoretical extreme case, could lead to further reductions in natural N₂O emissions through the year 27 2100. However, not enough is known about global natural N₂O emissions to justify changing the future 28 emission rate for this analysis (Syakila and Kroeze, 2011).

- 29
- 30 Anthropogenic emissions of N_2O have been partitioned into agricultural (LULCC) and other
- 31 anthropogenic (primarily fossil fuel) sources, which have been further partitioned into animal production

1 and cultivation sources for years prior to 2006 (Syakila and Kroeze, 2011). We compute the global N₂O 2 emitted per area covered by crop or pasture in the year 2000 using these estimates. Our estimate for 3 vear 2010 N₂O emissions from agriculture, 4.3 TgN(N₂O)vr⁻¹, is at the lower end of previously reported values compiled by Reav et al. (2012), ranging from 4.2 to 7 TgN(N₂O)yr⁻¹. The year 2000 ratios of 4 5 emission per area are applied to future changes in crop or pasture area to compute future LULCC N₂O 6 emissions for all scenarios. This assumes no future trends in the rates per cultivated land area of the 7 major agricultural N sources: N fertilizer application and animal waste management (Svakila and 8 Kroeze, 2011). Our approach results in increased N₂O emissions from agriculture between years 2010 9 and 2100 for RCP2.6, RCP8.5, and the theoretical extreme case (Table 1). Emissions decrease during the 21st century in the RCP4.5 scenario and are about the same in 2100 as in 2010 for RCP6.0. 10

11

12 2.4 Radiative forcing calculations

13

14 Radiative forcing (RF) is the change in energy balance at the top of the atmosphere due to a change in a 15 forcing agent, such as an atmospheric greenhouse gas. It is a commonly used metric for comparison of a 16 diverse set of climate forcings and can be used to approximate a global surface temperature response (Forster et al., 2007). The different atmospheric lifetimes of the relevant trace gas and aerosol species 17 18 (listed in Fig. 2) means that a single model approach cannot easily capture changes in all the forcing 19 agents (Unger et al., 2010) and, therefore, a combination of models and methodologies are used here 20 (Fig. 2). Here we summarize the different methodologies for computing the RFs, while detailed 21 descriptions are given in Appendix B.

22

23 We adopt the IPCC AR5 (Myhre et al., 2013) definitions of adjusted RF and effective RF (ERF) and 24 calculate the adjusted RFs for each forcing agent (ERFs for aerosol forcings), relative to a preindustrial 25 state (year 1850), with modeled radiative transfer or previously published expressions. Our choice of 26 preindustrial reference year is constrained by the available land cover change datasets, which start in 27 1850. However, large-scale anthropogenic land cover change began centuries before 1850, and 28 preindustrial changes could have an additional impact on present day climate, perhaps accounting for 29 nearly 10% of historical anthropogenic global surface temperature change (Pongratz and Caldiera, 30 2012). In our study, the RF of LULCC relative to the year 1850 is then compared to the RFs of other anthropogenic activities, dominated by fossil fuel burning. RFs due to non-LULCC activities are 31

calculated in this study for RCP4.5 non-LULCC emissions with identical methodology to that used for
LULCC emissions. All future LULCC RFs are calculated assuming background concentrations of trace
gases and aerosols characteristic of RCP4.5. With this approach we can examine the impacts of the
range in projected LULCC on RF independent of other anthropogenic activities. Although we are not
able to report, for example, the RF of projected LULCC from the RCP8.5 scenario in the context of
RCP8.5 fossil fuel emissions. Using a different projection to provide the background concentrations
would modify the resulting LULCC RFs.

8

9 The RFs of greenhouse gases from LULCC are easily computed from changes in their atmospheric concentrations since the preindustrial period. Time-dependent changes in CO₂ and N₂O concentrations, 10 11 which are long-lived in the atmosphere, are calculated with simple, pulse-response function and box-12 model approaches, respectively. To model changes in O₃ concentrations from LULCC, which has a relatively short atmospheric lifetime, we use the CAM version 4 (Hurrell et al., 2013; Gent et al., 2011) 13 14 with online chemistry from the Model for Ozone and Related chemical Tracers (MOZART) (Emmons et 15 al., 2010) which simulates all major processes in the photochemical production and loss of O_3 . Our 16 model setup also includes changes in O₃ deposition rate due to LULCC impacts on LAI through the 17 vegetation dependence of the dry deposition rate. Results from these simulations also determine 18 changes in the lifetime of CH₄ due to LULCC emissions of NMHCs and NO_x.

19

20 Aerosol chemistry and dynamics are simulated on a global scale using CAM version 5 (Liu et al., 2011) 21 with the three-mode Modal Aerosol Model (MAM3) (Liu et al., 2012), including the two-moment 22 microphysical scheme (Morrison and Gettelman, 2008) and aerosol/cloud interactions for stratiform 23 clouds. Since models generally disagree on the magnitude of the aerosol effects we use the IPCC-AR5 24 central estimate aerosol direct and indirect ERFs for the year 2011 to estimate the total anthropogenic 25 aerosol forcing in the year 2010 and use our model results to determine the proportion of the total 26 anthropogenic aerosols effects due to LULCC. We then apply the same scaling to the aerosol effects in 27 all future scenarios. The impacts of the LULCC aerosol emissions, both direct effects and indirect 28 effects on clouds, are diagnosed online within CAM5. We do not attempt to isolate the RF of aerosols 29 from quick-responding cloud feedbacks within the model and the computed forcings that include these 30 feedbacks are more appropriately referred to as effective radiative forcings (ERF). For computing a 31 total forcing from LULCC we include the aerosol ERFs with the RFs of the remaining forcing agents.

1

LULCC activities change vegetation cover and type, affect forest canopy coverage, and alter wildfire activity, all of which impact land surface albedo. We compute these impacts using output from the CLM simulations with and without LULCC (Sect. 2.2). Monthly averages for solar radiation incident upon the surface (after accounting for attenuation by monthly average cloud cover) are multiplied by the surface albedo with LULCC and without LULCC for each model grid point. The RF equals the global annual average difference between the outgoing solar radiation with LULCC and without LULCC.

8

9 2.4.1 Uncertainties

10

11 The uncertainty in these RF estimates arises largely from the uncertainty in modeling the effects of 12 aerosols and modeling the impacts of climate, CO₂ changes, and LULCC on the carbon cycle. Our 13 model predicts less uptake of anthropogenic carbon in natural land ecosystems compared to other land 14 models, and thus could be underestimating the impact of land use on these regions (C. Jones et al., 2013. 15 We compute the uncertainty in the total anthropogenic RF for each forcing agent with additional 16 uncertainty associated with the partitioning of each RF into LULCC and other anthropogenic 17 contributions, and with future fire emissions (Appendix C). For emissions from the theoretical extreme 18 case we assume that our scaling assumptions (Sect. 2.3.1) are valid and do not introduce additional 19 uncertainty, although the level of understanding of how emissions would scale under such an extreme 20 scenario is low.

21

22 In addition to the uncertainties, there are a few shortcomings inherent in our approach. We do not 23 include many biogeophysical effects of LULCC, such as changes to surface latent and sensible heat 24 fluxes and to the hydrological cycle, that impact climate (DeFries et al., 2002; Feddema et al., 2005; 25 Brovkin et al., 2006; Pitman et al., 2009; Lawrence and Chase, 2010). In general, while important for 26 local or regional climate especially in the tropics (Strengers et al., 2010), these effects are considered 27 minor on a global scale (Lawrence and Chase, 2010) and are difficult to quantify using the RF concept 28 (Pielke et al., 2002). For the calculation of the many forcing agents that we do consider, our approach is 29 to treat each forcing separately, which could lead to differences in RFs between agents that are due 30 partly to methodology. For example, land cover changes and agricultural emissions were developed 31 jointly for each of the RCPs, but for use in terrestrial models, including CLM, the land cover change

1 projections were altered (Di Vittorio et al., 2014). This leads to inconsistent storylines between future 2 emissions computed by CLM (Sect. 2.2) and those taken directly from the RCP integrated assessment 3 model output (Sect. 2.3.1). Therefore, it is important to view the future RFs computed here as 4 comprising a broad range in possible outcomes, extended with the TEC, as opposed to precise results 5 corresponding to specific storylines for the future. Finally, the inhomogeneous distribution of forcing 6 from surface albedo changes and short-lived trace gas and aerosol species could lead to non-additive (A. 7 Jones et al., 2013), and highly variable local climate responses (Lawrence et al., 2012). Therefore, we 8 use the RF for our assessment of global-scale climate impacts and acknowledge the limits of the RF 9 concept for predicting the diverse and often local impacts of land use (Betts, 2008; Runyan et al., 2012).

- 10
- 11 **3 Results**
- 12

13 **3.1 Land use impacts on present day radiative forcing**

14

We estimate a RF in the year 2010 from LULCC of 0.9 ± 0.5 W m⁻², 40% (+/- 16%) of the present day total anthropogenic RF (Fig. 3, Table 2). By separating the total anthropogenic RF (sum of LULCC and other anthropogenic activities) into contributions by forcing agent we can compare our calculations to the central estimates of Myhre et al. (2013) (Fig. 3) and the reported RFs of van Vuuren et al. (2011) (Table 3). Our calculations of the total, present day, anthropogenic RF correspond closely to the van Vuuren et al. (2011) values.

21

22 The major contributors to the present-day LULCC RF are associated increases in atmospheric CO₂ and CH₄. Deforestation, driven largely by the demand for additional agricultural land, leads to an estimated 23 net decrease in global forest area of roughly 5.5 million km⁻² from 1850 to 2010 (Lawrence et al., 2012; 24 25 Fig. A1), and a transfer of carbon from the terrestrial biosphere into the atmosphere. Past studies report 26 a LULCC contribution to current CO₂ concentrations (either year 2000 or 2005) of 26 ppm (Matthews et 27 al., 2004), 22 to 43 ppm (Brovkin et al., 2004), ~45 ppm (Strassmann et al., 2008), and 17 ppm (Arora and Boer, 2010). After adjusting for the CO₂ fertilization feedback, we estimate a LULCC contribution 28 29 of 28 ppm CO₂ in the year 2010. Our approach results in a year 2010 CO₂ concentration of 399 ppm 30 (285 ppm preindustrial, 86 ppm fossil fuels, 28ppm LULCC), which overshoots the observed change in CO₂ over the same period by about 10% but is well within the range of values from the CMIP5 fully 31

coupled climate model experiment, 368 ppm to 403 ppm in 2005 (Friedlingstein et al., 2013). The
 overestimate is in this case attributable to uncertainty in the total LULCC CO₂ emissions and uncertainty
 regarding the airborne fraction of historical emissions.

4

Present day LULCC and non-LULCC anthropogenic activities each emit close to 150 Tg CH₄ annually
(van Vuuren et al., 2007), yet the RF from LULCC CH₄ is roughly double the RF from non-LULCC
CH₄ (Fig. 3). The RF of non-LULCC CH₄ is diminished relative to LULCC CH₄ by the concurrent
emission of non-LULCC NO_x, which leads to greater tropospheric ozone (O₃) production, an increase in
the oxidation capacity of the troposphere, and as a result, a 20% reduction in CH₄ lifetime with respect
to removal by reaction with OH (Appendix B3).

11

12 From CAM4 simulations of atmospheric chemistry we find that tropospheric O₃ increases from 192 Tg in 1850 to 304 Tg in 2010, when all anthropogenic activities are included. The O₃ increase of 112 Tg 13 14 falls within the range of previous estimates (Lamarque et al., 2005). Here we separate the increase in O_3 15 concentrations into a non-LULCC contribution, 87%, and a LULCC contribution, 13%. The large non-16 LULCC contribution is attributable to additional O₃ formation from NO_x emissions from fossil fuel burning sources. The contribution of LULCC to changes in O₃ combines several competing effects 17 18 (Ganzeveld et al., 2010) including attributed changes in biogenic emissions of volatile organic 19 compounds (virtually no contribution by historical LULCC on a global average) and reductions in 20 emissions from wildfires (Table 1). The increase in tropospheric O₃ from LULCC is partially 21 compensated for by a slight increase in the dry deposition of O₃ with LULCC (6%) between 1850 and 22 2010 as a result of the LULCC-enhanced O₃ concentration and despite the decrease in O₃ removal efficiency in deforested areas, similar to the findings of Ganzeveld et al. (2010). The small contribution 23 24 of LULCC to global "short-lived" O₃ concentrations is augmented by additional O₃ (2.5 DU in 2010) 25 produced in response to long-term increases in CH₄ (primary mode response; Appendix B2). The additional O_3 from this response accounts for 60% of the LULCC O_3 RF of 0.12 Wm⁻² in 2010. The 26 27 primary mode response O3 is less important for non-LULCC activities because of the smaller CH₄ 28 contribution from these activities.

29

We assume that long-lived greenhouse gases, CO_2 , CH_4 , and N_2O , with lifetimes on the order of years to centuries, are sufficiently well-mixed in the atmosphere that the forcing from these gases in spatially

homogeneous (Table 4). The lifetime of tropospheric O_3 is considerably shorter, on the order of weeks, meaning concentrations can vary spatially, becoming higher near areas of O_3 production and remaining below the global average in remote regions away from areas of O_3 production. The RF varies in space with the concentration, although, these heterogeneities are moderate for O_3 . The RF at 80% of grid points is within ± 0.07 Wm⁻² of the global mean RF (Table 4).

6

7 While the positive RF from non-LULCC greenhouse gas emissions is offset to some extent by 8 concurrent emissions of aerosols, LULCC contributes both increases and decreases in aerosol emissions 9 resulting in nearly neutral aerosol RFs for the present day (Fig. 3). These opposing contributions to 10 aerosol emissions are evident in the spatial variability in AOD attributable to historical LULCC, ranging 11 between -0.18 to 0.29 (Table 4). Global average aerosol optical depth (AOD) is greater in 2010 and in 12 2100 for the RCP4.5, RCP6.0 and TEC scenarios when LULCC emissions are included, and lower for 13 RCP2.6 and RCP8.5 scenarios, but in all cases the attributed share of LULCC is less than 0.01. The RF from aerosol deposition onto snow and ice surfaces is negligible on a global average $(0.01 \text{ Wm}^{-2} \text{ for})$ 14 historical LULCC) but exceeds $\pm 1 \text{ Wm}^{-2}$ in some locations (Table 4). We also consider the impacts of 15 16 aerosols and trace gas species on atmospheric CO₂ due to bio-fertilization by deposition of P, Fe and N emitted from fires, and N from agriculture (NH₃, NO_x, N₂O). For present day emissions of these species 17 from LULCC activities (and land cover change impacts on fires), the drawdown of CO₂, enhanced 18 particularly by agricultural emissions of N, leads to a negative RF of -0.10 Wm⁻² that nearly 19 compensates for the positive RF from the greenhouse effect of agricultural N₂O emissions (0.14 Wm⁻²). 20 a noteworthy aspect of agricultural emissions that was also suggested by Zaehle et al. (2011). 21 22

Estimates for the global RF from albedo changes range from -0.10 (Skeie et al., 2011) to -0.28 W m⁻² 23 24 (Lawrence et al., 2012), with a substantial percentage, potentially 25%, caused by preindustrial LULCC 25 (Pongratz et al., 2009). Further estimates (Betts, 2001; Betts et al., 2007; Davin et al., 2007) fall near the IPCC AR5 central estimate of -0.15 Wm⁻² (Myhre et al., 2013). The RF from albedo changes is near 26 zero in most locations but has a high magnitude, up to 5 Wm^{-2} , in some localities on an annual average 27 28 (Table 4), similar to the findings of Betts et al. (2007). Our estimate for the global RF from historical land surface albedo change, -0.05 Wm⁻², is at the higher end of the range of previously published 29 30 estimates, yet still within the 90% confidence interval around the central estimate of Myhre et al. (2013). 31 Reductions in fire area burned that result from historical LULCC act to decrease the magnitude of the

surface albedo change forcing, although by less than 0.01 Wm⁻² for the present day. The use of a less
 altered, more natural background state than our year 1850 landscape would likely increase the
 magnitude of this forcing (Sitch et al., 2005; Pongratz et al., 2009).

4

5 **3.2** Future land use impacts on radiative forcing

6

7 In the year 2100 the RF attributable to anthropogenic LULCC, as projected by the RCPs, ranges between 0.9 to 1.9 Wm⁻² (Fig. 4), although as a percentage of the projected total anthropogenic RF (as 8 computed for RCP4.5), land use is less important in year 2100 than in 2010 (Table 2). Despite 9 10 diverging trajectories for forest area and crop area for RCP2.6, RCP4.5 and RCP6.0 in the 21st century (Fig. A1), the year 2100 LULCC RFs are similar between these scenarios (Fig. 4). The RCP8.5 RF is 11 12 characterized by relatively high contributions from CO₂ and CH₄ resulting in a total LULCC RF that is 13 double the average of the other three RCP scenarios. The difference between RCP8.5 and the other 14 scenarios suggests that decisions regarding global land policy similar to those used to develop the RCPs could reduce or increase global anthropogenic RF by 1 Wm⁻² by 2100. 15

16

The LULCC projections for all four RCP scenarios include future decreases in global deforestation rates 17 compared to recent historical rates (Fig. 5). A recent satellite assessment of global forest area gain and 18 loss reported a global forest loss rate of 12.5 Mha yr⁻¹ between 2000 and 2012 (Hansen et al., 2013), 19 suggesting the census-reported rates for 2000 to 2010 (FAO, 2010) may be estimating less deforestation 20 21 than is really occuring. If recent rates of observed forest area change persist, the global forest area 22 projected in all four RCP scenarios by Hurtt et al. (2011) will become overestimates in the near future, especially in RCP4.5 and RCP6.0. More extreme land use scenarios are plausible, and would have a 23 24 larger effect on climate. The theoretical extreme case, in which all arable land is converted to 25 agricultural land and all remaining land that is pasturable is converted to grasses by the year 2100, does 26 not take some important agricultural factors, such as changes in crop yields and per capita caloric intake, 27 into account, but was created to represent a limit to cropland expansion on Earth. Since we designate 28 arable land using a measure of climate suitability (Appendix A), following Ramankutty et al. (2002), 29 crop area could conceivably expand beyond this limit with the use of irrigation. In fact, areas of South 30 Asia currently support more agriculture than estimates of climate suitability suggest they should 31 (Ramankutty et al., 2002).

1

2 In the theoretical extreme case, crop area roughly doubles by the year 2050, and continues to increase at 3 the same rate to 2100. The rate of deforestation required to accommodate the expanded agriculture is 4 three times greater than upper estimates from the RCPs for year 2000-2030 forest loss (Fig. 5), resulting 5 in the near complete removal of tropical forests by the year 2100 (Fig. A2), and a global release of \sim 500 6 PgC from vegetation to the atmosphere. Loss of soil carbon often accompanies forest conversion to 7 crops or grasses (Lal, 2004) but this process is not well simulated in this generation of terrestrial models. 8 House et al. (2002) estimate terrestrial carbon loss from a complete deforestation to be between 450 to 9 820 PgC, with much of the uncertainty in the range due to different estimates of carbon loss from soils. 10 The version and configuration of CLM used in this study does not include the process of carbon loss 11 from soils from cultivation. Still, loss of carbon from vegetation alone in the theoretical extreme case 12 corresponds to roughly two-thirds of the value of the proven reserves of fossil fuels (760 PgC) (Meinshausen et al., 2009). The substantial loss of terrestrial carbon to the atmosphere in the theoretical 13 extreme case leads to a RF of 1.3 Wm^{-2} for CO₂ (Fig. 4). The magnitudes of all other forcing agents are 14 enhanced in this scenario, leading to a sum RF of 3.9 ± 0.9 Wm⁻² at the year 2100. 15

16

17 4.3 Enhancement of land use CO₂ radiative forcing

18

19 On average over all converted land types and land management histories, CO₂ RF from LULCC is 20 enhanced by the accompanying (although not necessarily concurrent) emissions of non-CO₂ greenhouse 21 gases and aerosols, such that the total RF is 2 to 3 times that of the CO₂ alone. For example, we estimate the net carbon flux from LULCC between 1850-2010 to be 140 PgC, leading to a RF from CO₂ 22 of ~0.4 W m⁻² in 2010, or about half of the total LULCC RF. In contrast, for other anthropogenic 23 activities the RF from CO₂ and the total RF are roughly equal (Fig. 3, Fig. 4). Therefore, while LULCC 24 25 accounted for about 20% of anthropogenic CO₂-equivalent emissions in 2010 (Tubiello et al., 2013), its 26 contribution to the anthropogenic RF is 40% (+/- 16%). We can express this enhancement factor as the 27 ratio of the sum RF to the CO₂ RF for LULCC, divided by the same ratio for other anthropogenic 28 activities (FF+), or $E = (RF_{sum}/RF_{CO2})_{LULCC}/(RF_{sum}/RF_{CO2})_{FF+}$. For all future LULCC scenarios the 29 enhancement factor is between 2.0 to 2.9 (Table 5). We compute the maximum enhancement of the CO₂ 30 RF for the RCP4.5 scenario (E = 2.9). In the development of the RCP4.5 scenario, international carbon trading incentivizes preservation of forests and reforestation, which reduces CO₂ emissions and the 31

1 resulting CO₂ RF from LULCC, increasing the enhancement factor.

2

3 The uncertainties in this factor (computed using the monte carlo method are described in Appendix C3) 4 are large but suggest that the enhancement is unlikely to be less than 1.3 for the year 2010 or any of the 5 given future scenarios. Values above 4.0 for the enhancement factor are within the uncertainty range for 6 the RCP4.5, RCP8.5 and TEC scenarios. The large enhancement factors for the RCP8.5 and TEC 7 scenarios result mainly from the substantial CH₄ RF relative to the CO₂ RF. For RCP4.5, this is a 8 reflection of the low CO₂ RF attributed to LULCC and relatively high total RF with contributions from 9 all other non-CO₂ greenhouse gases. The aerosol forcings play a minor role in the sum RF attributed to LULCC but impact the enhancement factor by reducing the non-LULCC forcing considerably. The 10 11 aerosol ERFs are the source of much of the uncertainty surrounding the enhancement factor. Since the RF calculations presented here are within uncertainty estimates across many models and estimates (Fig. 12 3), it is likely that other models or approaches would obtain similar results if the same processes and 13 14 activities were considered. We do not expect that the LULCC activities and biogeophysical forcings that 15 we exclude from this study would have a substantial impact on the enhancement as these forcings have 16 been shown to be small when considered on a global scale (Lawrence and Chase, 2010). Including model representation of LULCC impacts on soil carbon could increase the CO₂ and total RF attributed 17 18 to LULCC (Levis et al., 2014) and lead to a small reduction in the enhancement factors compared to the 19 values we report.

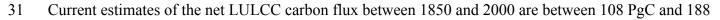
20

21 **5.** Conclusions

22

Effective strategies for mitigation of human impacts on global climate require an understanding of the major sources of those impacts (Unger et al., 2010). Anthropogenic land use and changes to land cover have long been recognized as important contributors to global climate forcing (Feddema et al., 2005), and yet most studies on this topic focus on either land use (e.g. Unger et al., 2010) or land cover change (e.g. Davin et al., 2007; Pongratz et al., 2009), but not both. In this study we compute the fraction of anthropogenic RF that is attributable to LULCC activities including a more comprehensive range of forcing agents.

30



1 PgC (Houghton, 2010), while here we estimate 131 PgC. Estimates from this study using the future 2 scenarios analyzed in the IPCC (the representative concentration scenarios or RCPs) suggest between 20 3 and 210 carbon will be released, consistent with Strassmann et al. (2008), and at the higher end of the 4 model range reported by Brovkin et al. (2013). Our model underpredicts the uptake of land carbon 5 relative to other models (e.g Arora et al., 2013), and unlike other estimates includes the explicit interplay 6 between changes in land use and fires (e.g. Marlon et al., 2008; Kloster et al., 2010). The RCP scenarios 7 were designed to cover a diverse set of pathways and create a broad range in possible outcomes for the 8 next century (Moss et al., 2010). Given that the RCP scenarios all project decreases in global forest area 9 loss rates in the 21st century relative to current rates, these scenarios are likely to be lower bounds on 10 deforestation rates in the future (Fig. 5). To explore higher rates of global forest loss and crop and 11 pasture expansions, we introduce a theoretical extreme case, in which all the arable land is converted to 12 agriculture and pasture usage by 2100. Since the rates of deforestation in this scenario are higher than current rates, this scenario is an upper bound on what could occur. We calculate that with the intense 13 14 pressures on land inherent to this scenario, between 590 and 700 PgC would be released from LULCC in 15 this century.

16

We find that the total RF contributed by LULCC is two to three times the RF from CO₂ alone when 17 additional positive forcings from non-CO₂ greenhouse gases and relatively small forcings from aerosols 18 19 and surface albedo are considered. The RF of other anthropogenic activities (largely fossil fuels) in 20 2010 and in 2100 (RCP4.5), relative to 1850, includes a large magnitude negative aerosol forcing that 21 offsets enough of the warming contribution from greenhouse gases that the total RF matches closely 22 with the RF from CO₂. The result of this enhancement of the LULCC RF with respect to its CO₂. 23 emissions, and lack of enhancement of the other anthropogenic activities RF, is a 40% LULCC 24 contribution to present day anthropogenic RF, a substantially larger percentage that is deduced from 25 greenhouse gas emissions alone (Tubiello et al., 2013). The percentage of anthropogenic RF attributable 26 to LULCC activities is likely to decrease in the future, even as the magnitude of the RF could increase by up to 1.0 Wm⁻² from 2010 to 2100. The lifetime and distribution of short-lived species makes 27 28 simplification difficult in terms of equating CO₂ RF to other constituents (Shine et al., 2007), but simple 29 approaches of controlling cumulative carbon (Allen et al., 2009) should account for the two to three 30 times enhancement of the LULCC RF over long time periods per unit CO₂ emitted relative to other 31 sources of CO₂.

1

2 Including forcings from aerosols in our assessment, while only slightly affecting the mean estimate of 3 the total LULCC RF, greatly increases the uncertainty in the estimate. Much of the uncertainty arises 4 from the simulation of aerosol/cloud interactions and the indirect effect for which very little model 5 consensus exists on a global scale (Forster et al., 2007). In addition to these uncertainties, the 6 perturbations of natural aerosol emissions by LULCC activities (mineral dust, SOA, wildfire smoke) are 7 only beginning to be better understood on a global scale (Ginoux et al., 2012; Ganzeveld et al., 2010). 8 Further research into the sources and lifetimes of natural aerosols, and anthropogenic impacts on their 9 emissions, could efficiently reduce our uncertainty in the contribution of LULCC to global RF. 10 11 While it is likely that advances in, and proliferation of, agricultural technologies will be sufficient to 12 meet global food demand without such an extreme increase in crop and pasture area, investment in foreign lands for agriculture, as a cost-effective alternative to intensification of existing agriculture, may 13 14 be hastening the conversion of unprotected natural lands (Rulli et al., 2013). Given the huge potential for climate impacts from LULCC in this century, estimated here to be 3.9 ± 0.9 Wm⁻² at the maximum, 15 16 similar to some estimates of future climate impacts from fossil fuels (e.g. Van Vuuren et al., 2011), our

17 study substantiates that not only energy usage but land use and land cover change needs to remain a

18 focus of climate change mitigation.